

## Reduced temperature-quenching of photoluminescence from indium nitride nanotips grown by metalorganic chemical vapor deposition

Shih-Chen Shi, Chia-Fu Chen, Geng-Ming Hsu, Jih-Shang Hwang, Surojit Chattopadhyay, Zon-Huang Lan, Kuei-Hsien Chen, and Li-Chyong Chen

Citation: *Applied Physics Letters* **87**, 203103 (2005); doi: 10.1063/1.2128484

View online: <http://dx.doi.org/10.1063/1.2128484>

View Table of Contents: <http://scitation.aip.org/content/aip/journal/apl/87/20?ver=pdfcov>

Published by the [AIP Publishing](#)

---

### Articles you may be interested in

High optical quality polycrystalline indium phosphide grown on metal substrates by metalorganic chemical vapor deposition

*J. Appl. Phys.* **111**, 123112 (2012); 10.1063/1.4730442

Photoluminescence properties of ZnO nanoneedles grown by metal organic chemical vapor deposition

*J. Appl. Phys.* **104**, 064311 (2008); 10.1063/1.2980335

Studies of InGaN GaN multiquantum-well green-light-emitting diodes grown by metalorganic chemical vapor deposition

*Appl. Phys. Lett.* **85**, 401 (2004); 10.1063/1.1773371

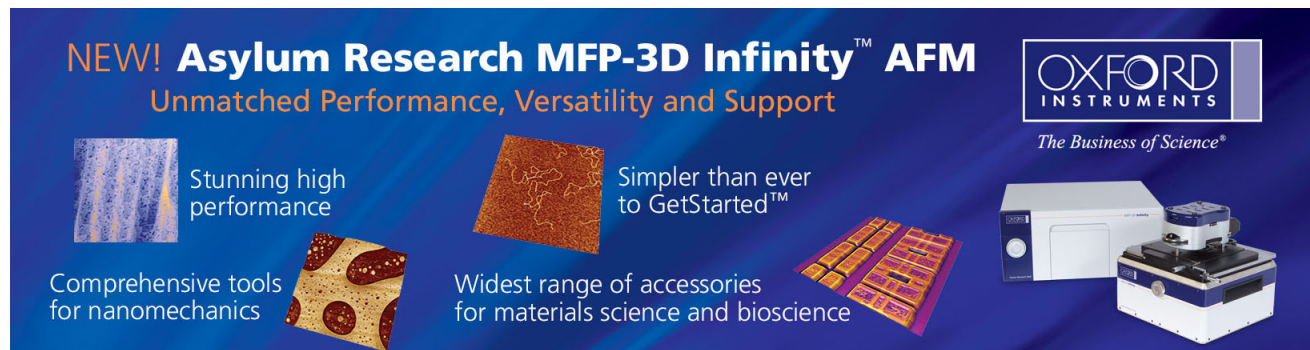
InGaN self-assembled quantum dots grown by metalorganic chemical-vapor deposition with indium as the antisurfactant

*Appl. Phys. Lett.* **80**, 485 (2002); 10.1063/1.1433163

Effects of growth interruption on the optical and the structural properties of InGaN/GaN quantum wells grown by metalorganic chemical vapor deposition

*J. Appl. Phys.* **90**, 5642 (2001); 10.1063/1.1410320

---

The advertisement features a dark blue background with white and orange text. At the top left, it reads 'NEW! Asylum Research MFP-3D Infinity™ AFM' in large white letters, followed by 'Unmatched Performance, Versatility and Support' in orange. On the right, the Oxford Instruments logo is shown with the tagline 'The Business of Science®'. Below the text are four images: a blue textured surface, a brown textured surface, a grid of small yellow and red squares, and a photograph of the MFP-3D Infinity AFM instrument. Text descriptions are placed around these images: 'Stunning high performance' next to the blue surface, 'Simpler than ever to GetStarted™' next to the brown surface, 'Comprehensive tools for nanomechanics' next to the grid, and 'Widest range of accessories for materials science and bioscience' next to the instrument photo.

## Reduced temperature-quenching of photoluminescence from indium nitride nanotips grown by metalorganic chemical vapor deposition

Shih-Chen Shi and Chia-Fu Chen

Department of Materials Science and Engineering, National Chiao Tung University, Hsinchu 300, Taiwan, Republic of China

Geng-Ming Hsu and Jih-Shang Hwang

Institute of Optoelectronic Sciences, National Taiwan Ocean University, Keelung 202, Taiwan, Republic of China

Surojit Chattopadhyay, Zon-Huang Lan, and Kuei-Hsien Chen

Institute of Atomic and Molecular Sciences, Academia Sinica, Taipei 106, Taiwan, Republic of China

Li-Chyong Chen<sup>a)</sup>

Center for Condensed Matter Sciences, National Taiwan University, Taipei 106, Taiwan, Republic of China

(Received 24 June 2005; accepted 14 September 2005; published online 8 November 2005)

We report metalorganic chemical vapor deposition of indium nitride (InN) nanotips with apex angles of  $10^\circ$  and length and base diameter of around  $1\ \mu\text{m}$  and  $200\ \text{nm}$ , respectively. The structure of the hexagonal InN nanotips growing along [002] was studied by electron microscopy and x-ray diffraction, and the optical properties were studied using temperature-dependent photoluminescence (PL) measurements. A narrow emission peak with a  $18\ \text{meV}$  full width at half maximum positioned at  $0.77\ \text{eV}$  was obtained with no visible emission. A PL quenching of only 14% was observed with a temperature scan of  $15\text{--}320\ \text{K}$ . © 2005 American Institute of Physics. [DOI: 10.1063/1.2128484]

Indium nitride (InN) is a key element in InGaN-based light emitting diodes (LEDs)<sup>1,2</sup> and also for high speed electronics<sup>3</sup> owing to its low electronic effective mass and high mobility.<sup>1,2</sup> However, the recent controversy about the fundamental band gap of InN has generated renewed interest in the material. The initial estimation at near  $1.9\ \text{eV}$ <sup>4</sup> has been challenged by Davydov *et al.*<sup>5</sup> suggesting it to be near  $0.7\ \text{eV}$  evident from photoluminescence (PL) measurements and absorption spectroscopy. Several other reports have confirmed such finding<sup>6,7</sup> and the apparent band gap near  $1.9\ \text{eV}$  was generally ascribed to the contribution from indium oxide related phase in the sample.<sup>5</sup> Other possible origins for the visible emission are the quantum size effect,<sup>8</sup> the Burstein–Moss shift<sup>9</sup> and nitrogen excesses in InN.<sup>10</sup> InN thin films have been prepared by several routes including metalorganic chemical vapor deposition (MOCVD), molecular beam epitaxy, chemical beam epitaxy, and vapor phase epitaxy.<sup>11</sup> The window for the growth temperature is narrow because of nitrogen dissociation from InN around  $550\ ^\circ\text{C}$ . Reports on nanostructured InN are scarce. InN nanoparticles<sup>12</sup> and nanowires<sup>13–15</sup> have been reported by the wet chemical synthesis and vapor-liquid-solid (VLS) routes. Recently, there has been a report on InN nanotube synthesis by a controlled carbonitridation reaction.<sup>16</sup> The scarcity of reports suggests that there are challenges involved in growing good quality InN nanostructures. This letter describes the MOCVD of single crystalline InN ‘nanotips’ (InNNTs) and evaluates the structural quality and the optical behavior of the material.

InNNTs were grown by the resistively heated MOCVD on gold (2 nm) coated quartz substrates held at  $550^\circ\text{C}$  and 50 Torr pressure for 90 min.<sup>17</sup> Epi-grade tri-methyl indium (EP-ICHEM, UK) and high purity (99.999%) ammonia were

used as growth precursors and high purity nitrogen was used as a carrier gas. Figure 1 shows a series of InNNT images taken collectively by high resolution scanning electron microscopy (JEOL 5700F HRSEM) [Figs. 1(a), 1(b), and 1(c)] and high resolution transmission electron microscopy [HRTEM/ JEOL JEM 4000 EX] [Figs. 1(e) and 1(f)]. The sharply faceted, hexagonal InNNTs growing along [002] are shown to carry a catalyst (Au in this case) at its apex which is less than  $10\ \text{nm}$  in diameter [1(b)] and having an apex angle of  $\sim 10^\circ$ . To our knowledge this is the first observation of solid InN nanotips, whereas that reported by Yin *et al.*<sup>16</sup> was a tubular form of InN. The schematic of the individual

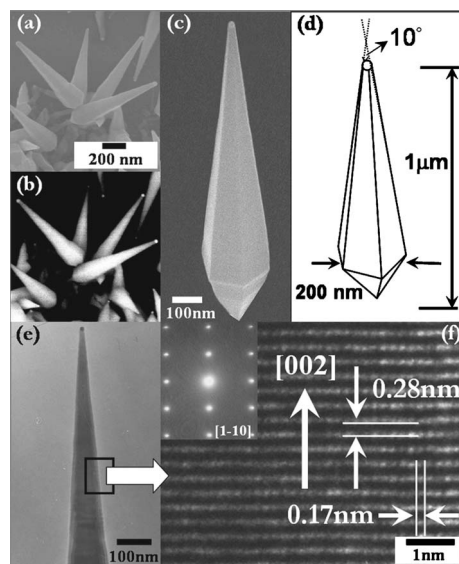


FIG. 1. (a) SEM image and (b) backscattered SEM image of InN nanotips; (c) low magnification SEM image and (d) schematic diagram of a single InN nanotip; (e) low magnification TEM image of a single nanotip and (f) HRTEM of the InN nanotip area marked in (e); inset showing the selected area diffraction pattern of *h*-InN nanotip.

<sup>a)</sup> Author to whom correspondence should be addressed; electronic mail: chenlc@ccms.ntu.edu.tw

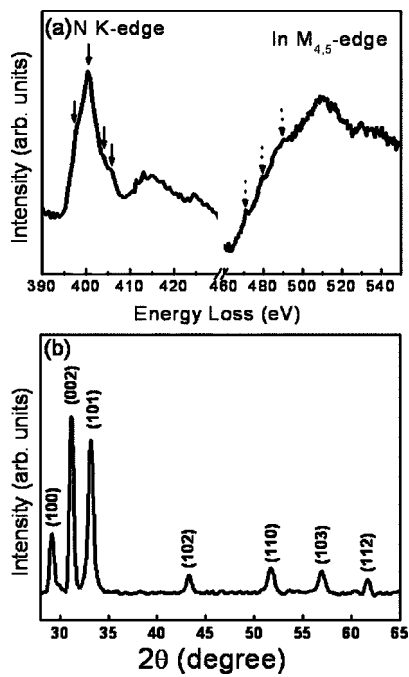


FIG. 2. (a) EELS result showing the N-K edge and the In  $M_{4,5}$ -edge spectra for the InN nanotips; (b) the x-ray diffraction spectrum of the InN nanotips showing the hexagonal signature.

InNNT [Fig. 1(d)] shows its representative dimensions. The selected area electron diffraction (SAED) of the InNNT [inset, Fig. 1(f)] also speaks of the good quality single crystalline hexagonal phase. The presence of polycrystalline InN grains, which can complicate the interpretations of the PL data presented later, can be ruled out from the observed SAED pattern [inset, Fig. 1(f)] and the HRTEM images [Figs. 1(e) and 1(f)].

The composition of the InNNTs has been established from electron energy loss spectroscopy (EELS). The nitrogen K edge and the In  $M_{4,5}$  edges, along with the fine structures,<sup>18</sup> were clearly seen in EELS data [Fig. 2(a)]. Further information on the structural quality of the InNNTs can be obtained from the x-ray diffraction (XRD) (Rigaku DMAX/C x-ray diffractometer). The XRD spectrum [Fig. 2(b)] shows signature peaks of the hexagonal InN phases (Joint Committee for Powder Diffraction Standards, card No. 02-1450).

The infrared (IR) range PL was taken from a conventional PL setup equipped with an InGaAs detector using Argon 488 and 514 nm line for excitation. The PL spectra of the InNNTs measured with 488 nm laser and a 3 mm slit on the detector path are shown in Fig. 3(a). A sharp emission peak at 0.77 eV<sup>5,6</sup> was observed with a linewidth full width at half maximum of 18 meV with no significant emission around the visible. A weak peak near 0.754 eV may be due to 20-meV-deep donor level in InN.<sup>19</sup> The peak at  $\sim 0.735$  eV could not be assigned at the present. Temperature dependence of the IR-PL peak measured with an incident laser power of 100 mW shows less than 14% (factor of 1.15) decrease in the emission intensity when the temperature was varied from 15 to 300 K [open squares, Fig. 3(b)]. The PL efficiency ( $\eta$ ) defined as the ratio of the radiative transition probability ( $P_r$ ) and the sum of radiative and nonradiative transition probabilities, can be written as<sup>20</sup>

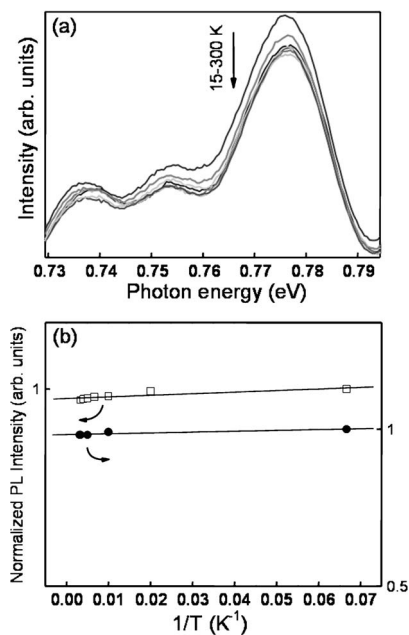


FIG. 3. (a) The temperature dependent PL spectra of InN nanotips measured with 100 mW incident laser power and 3 mm slit width. (b) Two sets of Arrhenius plot of the normalized integrated photoluminescence intensity as a function of inverse temperature: (□) 15–300 K, 488 nm laser, 3 mm slit width (■) 15–320 K, 514 nm laser, 0.5 mm slit width.

$$\eta = \frac{P_r}{[P_r + {}^A P_{nr} + {}^B P_{nr}]}, \quad (1)$$

where  ${}^A P_{nr}$  and  ${}^B P_{nr}$  are transition probabilities for two non-radiative mechanisms in different temperature regimes. The temperature dependence of the nonradiative transition probabilities can be written as

$${}^X P_{nr} = X \exp\left(-\frac{E_X}{\kappa T}\right) \quad (2)$$

with  $X=A$ , or  $B$ , where  $E_A$  and  $E_B$  are the thermal activation energies for the two processes, and  $A$  and  $B$  are temperature independent prefactors. The temperature dependent efficiency can hence be written as

$$\eta(T) = \frac{1}{\left[1 + \frac{A}{P_r} \exp\left(-\frac{E_A}{\kappa T}\right) + \frac{B}{P_r} \exp\left(-\frac{E_B}{\kappa T}\right)\right]}. \quad (3)$$

Here,  $P_r$  is assumed to be independent of temperature. Assuming the efficiency,  $\eta$ , to be solely governing the PL intensity and that  $\eta(15 \text{ K})=100\%$ , a high internal efficiency at room temperature can be estimated from Fig. 3. Indication about the magnitude of the activation energies ( $E_A$  and  $E_B$ ) can be obtained from the Arrhenius plot of the normalized PL intensity as a function of inverse temperature [Fig. 3(b)] and its linear fit according to Eq. (3). Generally, two distinct regions, one with a high activation near room temperatures and another with low activation at low temperatures, were obtained. Two features stand out from Fig. 3(b). First, is the extremely small value of the activation energy ( $E_A < 6$  meV) at low temperatures that supports the assumption ( $\eta(15 \text{ K})=100\%$ ) made earlier. Second, is the absence of the PL quenching near room temperature, which, when present, will give rise to the second region with a high thermal activation energy ( $E_B$ ). For multiple quantum wells, such

as InGaP/AlGaInP, the thermal activation energy  $E_A$  accounts for loss mechanism within the well, whereas  $E_B$  accounts for carrier emission outside the well followed by nonradiative recombination in the barriers.<sup>21</sup> The small activation energy ( $E_A$ ) below room temperature can be attributed to excitonic binding energy with impurities. But Lambkin *et al.*<sup>20</sup> specified  $E_A$  to be responsible for carriers thermalizing from localized regions of order induced band edge fluctuations in InGaP materials. In some cases the activation energy,  $E_B$ , was attributed to nonradiative recombination in the dislocations.<sup>22</sup>

The absence of the room temperature PL quenching was somewhat unusual and double checked with a 514 nm excitation and a 0.5 mm slit on the detector path. The narrowing of the slit width did reduce the overall intensity of the 0.77 eV line but the temperature dependence carried out from 15 to 320 K, in this case, showed a similar absence of quenching [filled circles, Fig. 3(b)] and a small activation energy of 5.2 meV. In comparison, the GaAsSb/GaAs quantum wells showed a marked PL quenching measured in the same PL instrumental setup.<sup>23</sup> Also InN films show a marked quenching in the vicinity of room temperature.<sup>24</sup> The features of Fig. 3 taken together speak of a high internal quantum efficiency in the InN material. Nonradiative recombination in defects, such as dislocations, is minimal. The absence of PL quenching near room temperature clearly indicates a minimum thermal escape of carriers from any confining potential within the InNNTs. We have already ruled out polycrystalline grains in the material that could account for nonradiative recombinations. Although we cannot ignore the presence of surface states in nanomaterials, clearly these surface states are not populated even at room temperature, because of a strong electron-hole coupling in the bulk. The surface states can again be passivated by a wide bandgap InO layer, on these InNNTs, blocking the thermal escape routes of the carriers due to large energy requirements. Even after the report of the IR band gap of InN there are reports that still support the visible 1.9 eV band gap of InN.<sup>16</sup> Many reports indicated that the visible band gap may be due to InO in the material.<sup>25</sup>

The absence of the visible PL in our case can be due to (i) absence of significant proportion of InN nanocrystals (<5 nm) that can shift the IR peak into the visible with the assumption of an ultrasmall electron effective mass ( $0.042 m_0$ ),<sup>8</sup> (ii) low carrier concentration in the crystal to minimize any Burstein–Moss shift<sup>9</sup> which has the ability to shift the band gap from 0.7 to 1.7 eV,<sup>26</sup> and (iii) absence of excess nitrogen in InN.<sup>10</sup> High-quality stoichiometric InN film with carrier concentration of high  $10^{17} \text{ cm}^{-3}$  and mobility in excess of  $1000 \text{ cm}^2 \text{ V}^{-1} \text{ s}^{-1}$  was reported to have PL emissions at 0.70 eV.<sup>27</sup> The other possibility of optical transitions between interface states of metallic In clusters in the InN matrix<sup>28</sup> can be effectively ruled out since we did not observe the In clusters in our TEM measurements. Moreover, if the In clusters were to dominate the PL measurements, its density must be high enough to be observable under TEM and XRD which is not the case in the present study as well as that reported.<sup>27</sup>

In summary, we have demonstrated the growth of solid indium nitride nanotips, with apex angles of  $10^\circ$  and lengths of  $1 \mu\text{m}$ , by metalorganic chemical vapor deposition at temperatures of  $550^\circ\text{C}$ . The VLS grown InN nanotips were found to be hexagonal with a [002] axial growth direction.

High resolution TEM demonstrated the nearly defect free structure of the nanotips corroborated by the weak quenching (<14%) of the 0.76 eV photoluminescence peak intensity over a 285 K temperature scan.

Support from Academia Sinica, NSC and MOE, Taiwan, and the U.S. Air Force of Scientific Research/Asian Office of Aerospace Research and Development is gratefully acknowledged. The authors thank Professor Y. F. Chen, National Taiwan University, for useful discussion and the use of the IR-PL setup.

<sup>1</sup>S. Chichibu, T. Azuhata, T. Sota, and S. Nakamura, *Appl. Phys. Lett.* **69**, 4188 (1996).

<sup>2</sup>K. P. O'Donnell, R. W. Martin, and P. G. Middleton, *Phys. Rev. Lett.* **82**, 237 (1999).

<sup>3</sup>B. E. Foutz, S. K. O'Leary, M. S. Shur, and L. F. Eastman, *J. Appl. Phys.* **85**, 7727 (1999).

<sup>4</sup>T. L. Tansley and C. P. Foley, *J. Appl. Phys.* **59**, 3241 (1986).

<sup>5</sup>V. Y. Davydov, A. A. Klochikhin, R. P. Seisyan, V. V. Emtsev, S. V. Ivanov, F. Bechstedt, J. Furthmuller, H. Harima, A. V. Mudryi, J. Aderhold, O. Semchinova, and J. Grual, *Phys. Status Solidi B* **229**, R1 (2002).

<sup>6</sup>J. Wu, W. Walukiewicz, K. M. Yu, J. W. Ager III, E. E. Haller, H. Lu, W. J. Schaff, Y. Saito, and Y. Nanishi, *Appl. Phys. Lett.* **80**, 3967 (2002).

<sup>7</sup>T. Matsuoka, H. Okamoto, M. Nakao, H. Harima, and E. Kurimoto, *Appl. Phys. Lett.* **81**, 1246 (2002).

<sup>8</sup>B. R. Nag, *Phys. Status Solidi B* **237**, R2 (2003).

<sup>9</sup>J. Wu, W. Walukiewicz, W. Shan, K. M. Yu, J. W. Ager III, E. E. Haller, H. Lu, and W. J. Schaff, *Phys. Rev. B* **66**, 201403 (2002).

<sup>10</sup>T. V. Shubina, S. V. Ivanov, V. N. Jmerik, M. M. Glazov, A. P. Kalvarskii, M. G. Tkachman, A. Vasson, J. Leymarie, A. Kavokin, H. Amano, I. Akasaki, K. S. A. Butcher, Q. Guo, B. Monemar, and P. S. Kop'ev, *Phys. Status Solidi A* **202**, 377 (2005).

<sup>11</sup>A. G. Bhuiyan, A. Hashimoto, and A. Yamamoto, *J. Appl. Phys.* **94**, 2779 (2003).

<sup>12</sup>S. D. Dingman, N. P. Rath, P. D. Markowitz, P. C. Gibbons, and W. E. Buhro, *Angew. Chem., Int. Ed.* **39**, 1470 (2000).

<sup>13</sup>C. H. Liang, L. C. Chen, J. S. Hwang, K. H. Chen, Y. T. Hung, and Y. F. Chen, *Appl. Phys. Lett.* **81**, 22 (2002).

<sup>14</sup>K. Sardar, F. L. Deepak, A. Govindaraj, M. M. Seikh, and C. N. R. Rao, *Small* **1**, 91 (2005).

<sup>15</sup>J. Zhang, B. L. Xu, F. H. Jiang, Y. D. Yang, and J. P. Li, *Phys. Lett. A* **337**, 121 (2005).

<sup>16</sup>L. W. Yin, Y. Bando, D. Golberg, and M. S. Li, *Adv. Mater. (Weinheim, Ger.)* **16**, 1833 (2004).

<sup>17</sup>J. S. Hwang, C. H. Lee, F. H. Yang, K. H. Chen, L. G. Hwa, Y. J. Yang, and L. C. Chen, *Mater. Chem. Phys.* **72**, 290 (2001).

<sup>18</sup>K. A. Mkhoyan, J. Silcox, E. S. Allredge, N. W. Ashcroft, H. Lu, W. J. Schaff, and L. F. Eastman, *Appl. Phys. Lett.* **82**, 1407 (2003).

<sup>19</sup>S. Z. Wang, S. F. Yoon, Y. X. Xia, and S. W. Xie, *J. Appl. Phys.* **95**, 7998 (2004).

<sup>20</sup>J. D. Lambkin, L. Considine, S. Walsh, G. M. O'Connor, C. J. McDonagh, and T. J. Glynn, *Appl. Phys. Lett.* **65**, 73 (1994).

<sup>21</sup>E. M. Daly, T. J. Glynn, J. D. Lambkin, L. Considine, and S. Walsh, *Phys. Rev. B* **52**, 4696 (1995).

<sup>22</sup>A. Hangleiter, *Phys. Rev. B* **48**, 9146 (1993).

<sup>23</sup>Y. S. Chiu, M. H. Ya, W. S. Su, and Y. F. Chen, *J. Appl. Phys.* **92**, 5810 (2002).

<sup>24</sup>R. Intartaglia, B. Maleyre, S. Ruffenach, O. Briot, T. Taliercio, and B. Gil, *Appl. Phys. Lett.* **86**, 142104 (2005).

<sup>25</sup>M. Yoshimoto, H. Yamamoto, W. Huang, H. Harima, J. Saraie, A. Chayahara, and Y. Horino, *Appl. Phys. Lett.* **83**, 3480 (2003).

<sup>26</sup>J. Wu, W. Walukiewicz, S. X. Li, R. Armitage, J. C. Ho, E. R. Weber, E. E. Haller, H. Lu, W. J. Schaff, A. Barcz, and R. Jakiela, *Appl. Phys. Lett.* **84**, 2805 (2004).

<sup>27</sup>K. M. Yu, Z. Liliental-Weber, W. Walukiewicz, W. Shan, J. W. Ager III, S. X. Li, R. E. Jones, E. E. Haller, H. Lu, and W. J. Schaff, *Appl. Phys. Lett.* **86**, 071910 (2005).

<sup>28</sup>T. V. Shubina, S. V. Ivanov, V. N. Jmerik, D. D. Solnyshkov, V. A. Vekshin, P. S. Kop'ev, A. Vasson, J. Leymarie, A. Kavokin, H. Amano, K. Shimono, A. Kasic, and B. Monemar, *Phys. Rev. Lett.* **92**, 117407 (2004).